Journal of Materials Chemistry A

Accepted Manuscript

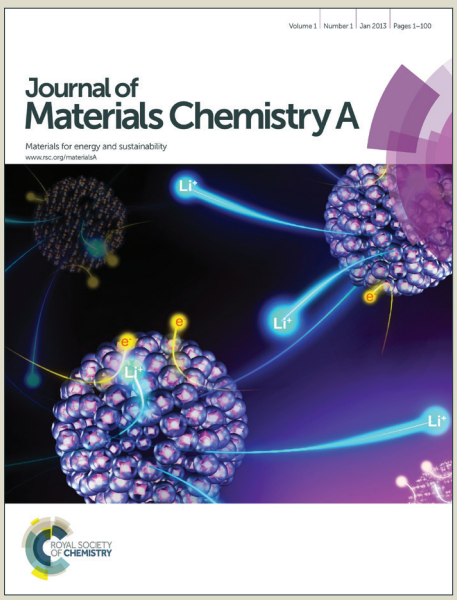

ROYAL SOCIETY OF CHEMISTRY

www.rsc.org/materialsA

Highly enhanced plasmonic photocatalytic activity of Ag/AgCl/TiO_2 by CuO co-catalyst

Zameer Hussain Shah[a], Jiasheng Wang[b], Yuzhen Ge[a], Cui Wang[a], Wenxin Mao[a], Shufen Zhang[a], and Rongwen Lu[a]*

[a]*State Key Laboratory of Fine Chemicals, Dalian University of Technology, Dalian 116024, People's Republic of China.*

[b] *State Key Laboratory of Fine Chemicals, School of Petroleum and Chemical Engineering, Dalian University of Technology, Panjin, Liaoning 124221, People's Republic of China.*

Author for Correspondence:

Rongwen Lu

State Key Laboratory of Fine Chemicals, Dalian University of Technology, Dalian 116024, People's Republic of China.

Fax: +86-411-84986292.

Tel: +86-411-84986270.

E-mail: lurw@dlut.edu.cn.

Abstract. The role of CuO as a co-catalyst was studied on plasmonic photocatalysis of Ag/AgCl/TiO_2 and it was found that the photocatalytic degradation of methyl orange and phenol under visible light was highly enhanced when CuO was incorporated into Ag/AgCl/TiO_2. The samples were characterized by X-ray diffraction (XRD), transmission electron microscopy (TEM), X-ray photoelectron spectroscopy (XPS), and UV/vis spectrophotometry. The photocatalytic activity under visible light was attributed to the SPR of Ag NPs and enhancement of this activity was achieved due to CuO which act as a sink for photogenerated electrons.

Keywords: Co-catalyst, Surface plasmon resonance, Visible light, TiO_2, Plasmonic photocatalysis.

1 Introduction

Titanium Dioxide (TiO_2) is believed to be the most promising photocatalyst to solve the environment and energy crises for the ever increasing demands[1-3]. Abundant availability, non-toxicity, and chemical stability make TiO_2 as one of the most promising materials for water purification, water splitting, solar cells, and so on[4-6]. However, TiO_2 is active only under UV light because of its wide band gap (3.2 eV). UV makes only about less than 5% of the sunlight so band gap tuning is desired to make TiO_2 active under the larger portion

of the solar spectrum.[7] Different approaches are being explored to achieve the visible light activation of TiO_2, e.g. anionic or cationic doping[8-10], coupling narrow band gap semiconductors as sensitizer[11], tuning morphology[12], and exploring localized surface plasmon resonance by plasmonic nanoparticles[13](NPs).

Noble metal (Au, Ag) NPs can strongly absorb visible light owing to the surface plasmon resonance (SPR) shown by them[14]. SPR is reported to play an important role in improving the photocatalytic performance of a semiconductor[15]. Among the plasmonic materials, Ag has been proposed to be the most important [16]. Silver NPs have been used to develop various plasmonic photocatalysts[17] e.g. Ag/TiO_2[13], Ag@AgCl[18], $Ag/AgCl/TiO_2$[17], Ag_2O/TiO_2[19] etc.

Apart from the above mentioned TiO_2 modifications, some rather unusual strategies have also been successfully exploited to enhance TiO_2 photocatalysis. These include using interfacial charge transfer (IFCT)[20], use of chirality to tune the incident light[21], increasing light absorption with black hydrogenated TiO_2[22], up-conversion by rare-earth doped luminescent material[23], and use of a co-catalyst[24] etc. A co-catalyst can enhance the photocatalytic activity of a semiconductor by (i) suppressing the charge recombination by trapping the photogenerated charges, (ii) improving the photostability of the catalyst by

timely consumption of photogenerated charges, particularly holes, and (iii) lowering the activation energy hence catalyzing the reactions[24]. Transition metal oxide nanoclusters of Cu(II)[25] and Fe(III)[26] have been reported as co-catalysts to enhance the photocatalytic activity of TiO_2. From these reports, we anticipated that plasmonic photocatalysis of TiO_2 can be further enhanced by the use of a co-catalyst. To the best of our knowledge, there has not been any report on the combined effect of SPR and a co-catalyst on TiO_2 photocatalysis.

Herein, we report a new kind of composite CuO/Ag/AgCl/TiO_2 which showed high photocatalytic activity for the visible light degradation of methyl orange (MO) and phenol. Photocatalytic degradation of dyes is generally studied as a model reaction to test the photocatalytic activity of a catalyst[27]. The CuO was found to greatly enhance the photocatalytic activity of Ag/AgCl/TiO_2 by acting as a co-catalyst. The photocatalyst was prepared by a reverse microemulsion method.

2 Materials and methods

2.1 Materials

Polyoxyethylene (20) cetyl ether (Brij-58) was purchased from Acros. Titanium (iv) isopropoxide (TTIP) was provided by J & K Chemical Ltd. Cyclohexane, silver nitrate

($AgNO_3$), copper nitrate trihydrate ($Cu(NO_3)_2 \cdot 3H_2O$), acetonitrile, ethanolamine (ETA), triethanolamine (TEA), sodium borohydride ($NaBH_4$), isopropyl alcohol (IPA), ethylene glycol (EG), calcium chloride ($CaCl_2$), phenol and methyl orange were all purchased from Sinopharm Chemical Reagent Co. Ltd. (SCRC). All chemicals were analytical grade and used without further purification. Deionized water (18.2MΩ) was used throughout the experiments.

2.2 Synthesis of CuO/Ag/AgCl/TiO_2

In a typical synthesis, 6.738 g of Brij-58 was taken in a two-neck flask. The temperature was kept at 50 °C throughout the experiment. Anhydrous $CaCl_2$ was added to EG to dehydrate it. 2 mL dehydrated EG was added to the melted Brij-58. 1.2 mL 0.5 M $AgNO_3$, complexed by 0.38 mL ETA and dissolved in acetonitrile was added. The solution turned milky showing the formation of AgCl. Then 0.05 mL 0.5 M $Cu(NO_3)_2 \cdot 3H_2O$, complexed by 0.025 mL TEA and dissolved in acetonitrile , was added and the solution turned into purple. The solution was evaporated to remove acetonitrile. 30 mL cyclohexane was added and stirred for 15 min, followed by the addition of 0.140 g $NaBH_4$. The solution turned to dark brown. After 30 min, 0.5 mL TTIP was added in successive additions of 0.2 mL, 0.15 mL, and 0.15 mL having a gap of 15 min each. After 1 h of the last TTIP

addition, 30 mL IPA was added and the precipitate was separated by centrifugation followed by washing with IPA and cyclohexane. The precipitate was dried at 100°C for 10 h and then calcined at 500°C for 2 h to obtain the powder.

2.3 Characterization

Morphological studies were carried out by transmission electron microscopy (TEM). TEM analysis was carried out at room temperature on a JEOL JEM-2000 EX transmission electron microscope using an accelerating voltage of 120 kV. High resolution TEM images were obtained on a JEM-2100F (JEOL) transmission electron microscope operated at 200 kV. The XRD pattern was recorded on a Rigaku DMAX IIIVC X-ray diffractometer with Cu-Kα (0.1542 nm) radiation scanning from 10° to 80° (2θ) at the rate of 6 °/min. XPS was acquired by VG ESCALAB 250 with an Al-Kα X-ray source operating at 150 W (15 kV). The binding energies were calibrated using the C 1s peak at 284.6 eV. The curve fitting was performed by XPS PEAK 4.1 software. UV/vis spectra were obtained by JASCO UV-550.

2.4 Photocatalytic Activity

0.040 g catalyst was added to a 50 mL MO solution (10 mg/L) in a beaker. The solution was stirred magnetically at 30 °C. Prior to irradiation, the solution was kept in dark for 30

min to achieve the adsorption-desorption equilibrium. The light source used was a Xe lamp (AULLT Cell-HFX300) equipped with a UV-cut off filter ($\lambda \geq 400$ nm). Visible light was irradiated on the solution and a 3 mL aliquot was taken at regular intervals of time. The photocatalytic activity was monitored by analyzing the aliquot samples on a UV-visible spectrophotometer (Agilent 8453) at 465 nm. For phenol degradation, 0.050g catalyst was added to a 50 mL phenol solution (20 mg/L) and degradation was monitored at 270 nm wavelength on the UV-visible spectrophotometer. Percent degradation (%D) of pollutant was calculated using the following equation:

$$\%D = (C_0 - C)/C_0 * 100\%$$

Where C_0 is the concentration before irradiation and C is the concentration at any sampling time.

3 Results and discussion

3.1 Characterization

$CuO/Ag/AgCl/TiO_2$ was synthesized in a reverse microemulsion system. The morphology of the obtained powder was determined by TEM images which revealed that the as synthesized powder did not have a regular morphology. Low resolution TEM image (Figure 1a) gave no distinction among the various components of the obtained

catalyst. While HR TEM image (Figure 1b) clearly showed the presence of different entities. The interplaner spacing of 0.31 nm corresponds to AgCl (101), 0.21 nm corresponds to CuO (200), 0.25 nm corresponds to Ag (004) , and 0.28 nm corresponds to TiO_2 (002). These findings were further confirmed by XRD. Figure 1c shows the XRD patterns of different catalysts synthesized during this study. The analysis of the pattern for CuO/Ag/AgCl/TiO_2 shows that the peaks can be indexed using TiO_2 anatase phase (JCPDS file no. 01-0562), TiO_2 rutile phase (JCPDS file no. 01-1292), AgCl (JCPDS file no. 22-1326), Ag (JCPDS file no. 41-1402), and CuO (JCPDS file no. 78-0428). All these observations are consistent with the TEM images.

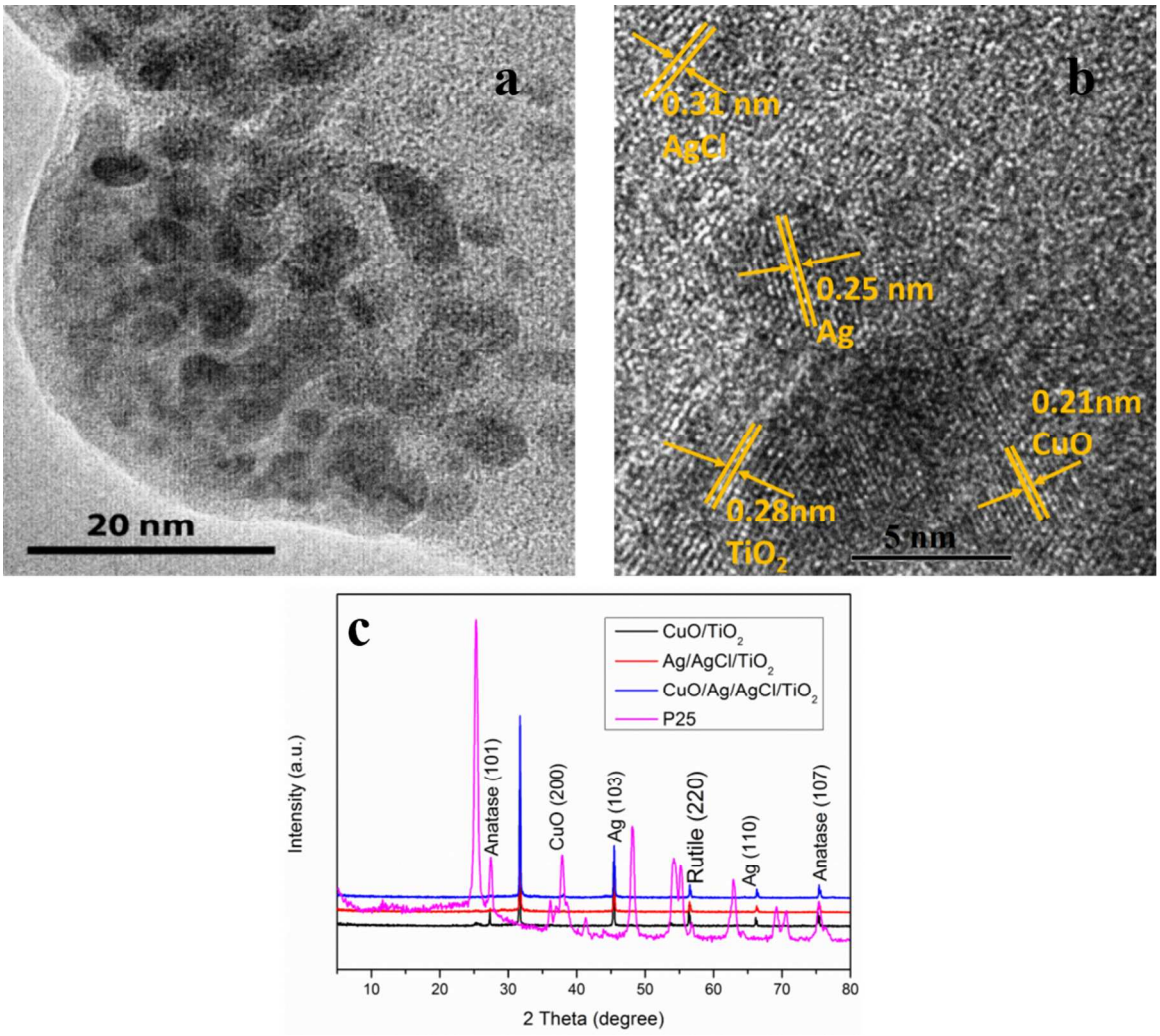

Figure 1: (a) Low magnification TEM image, (b) HRTEM image of CuO/Ag/AgCl/TiO_2, and (c) XRD patterns of different materials.

The elemental composition and chemical status were analyzed by XPS. Figure 2a shows the full range of the XPS spectrum for CuO/Ag/AgCl/TiO_2 revealing peaks for Cl, C, Ag, Ti, O, and Cu. XPS peaks show that Ag $3d_{5/2}$ at 367.0 eV and Ag $3d_{3/2}$ at 373.0 eV in Figure 2b belong to metallic Ag, while Ag $3d_{5/2}$ at 367.8 eV and Ag $3d_{3/2}$ at 373.8 eV

correspond to Ag(I) in AgCl[28]. Figure 2c demonstrates the high resolution XPS spectrum for Cl 2p which coresponds to AgCl, while the high resolution XPS spectrum of Cu 2p (Figure 2d) confirms the presence of Cu(II) and it coresponds to CuO.

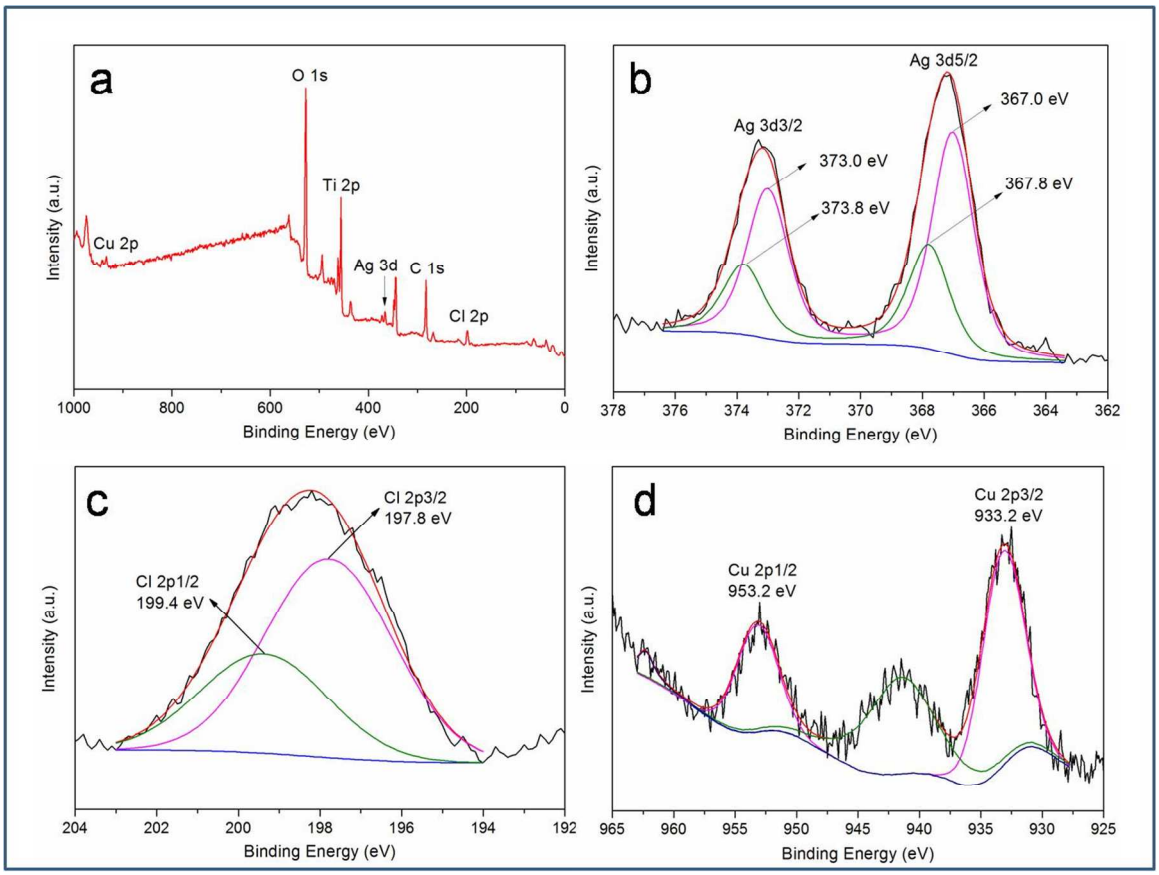

Figure 2: (a) XPS survey of CuO/Ag/AgCl/TiO_2, (b) Ag 3d scan (c) Cl 2p scan, and (d) Cu 2p scan.

Presence of Ag NPs was also confirmed by UV/vis spectra of both Ag/AgCl/TiO_2 and CuO/Ag/AgCl/TiO_2. As shown in Figure 3, there is a clear absorbance peak in the visible

region for both the mentioned samples. This peak can be attributed to the SPR associated with Ag NPs.

During the synthesis, AgCl was formed by the reaction between $AgNO_3$ and $CaCl_2$. Reduction was carried out by $NaBH_4$. Copper ions were also reduced to copper atoms during this reduction. These copper atoms were converted to CuO during the calcination in air. Synthesis reaction equations are given in the supporting information. All these species were confirmed from TEM, XRD, XPS, and UV/vis. Hence we conclude that $CuO/Ag/AgCl/TiO_2$ was successfully synthesized.

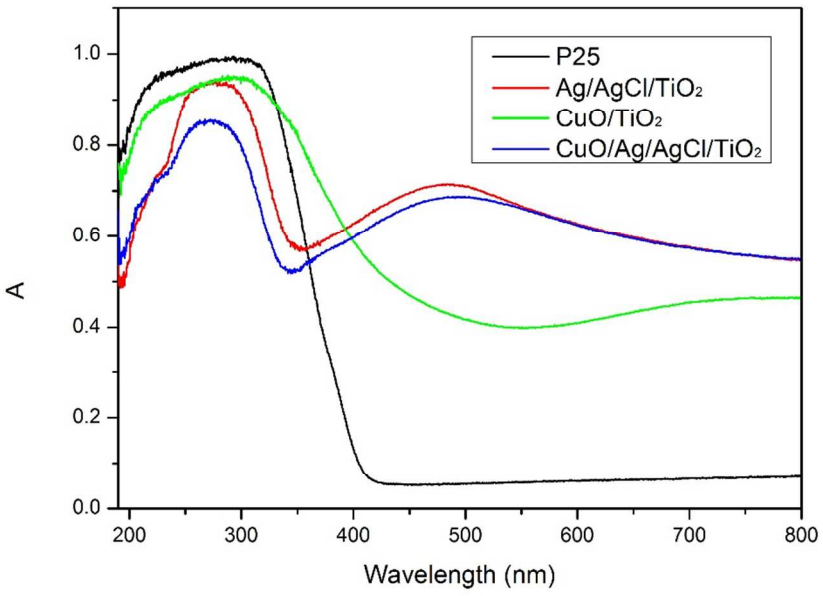

Figure 3: UV/vis spectra of different catalysts used.

3.2 Photocatalytic degradation of methyl orange (MO) and phenol over $CuO/Ag/AgCl/TiO_2$

The photocatalytic activity of the as synthesized catalysts was evaluated by the degradation of MO and phenol under visible light irradiation. MO concentration was decreased steadily in the presence of $CuO/Ag/AgCl/TiO_2$ (Figure 4a) under visible light irradiation. Figure 4a shows the %D by various catalysts under visible light. No color change was observed in the case of commercial TiO_2 (P25) and the as prepared CuO/TiO_2. Visible light is not energetic enough to excite electron in the case of P25 or CuO/TiO_2. Considerable color change was observed in the case of $Ag/AgCl/TiO_2$ and under our experimental conditions, a degradation of 42% was achieved in 25 min irradiation time. Photocatalytic degradation of MO was greatly enhanced in the case of $CuO/Ag/AgCl/TiO_2$. Under the same experimental conditions, 91% degradation was achieved in 25 min in the case of $CuO/Ag/AgCl/TiO_2$. In this case, the yellow colored MO solution became almost colorless in 20 min (Figure 4b inset).

For excluding the effect of photosensitization, degradation of colorless organic pollutant phenol was also studied under visible light in presence of the as synthesized catalysts. The results are depicted in Figure 4c and d. About 53% phenol degradation was achieved

in the case of Ag/AgCl/TiO_2 in 50 min while 71% degradation was achieved in the presence of CuO/Ag/AgCl/TiO_2. These results further confirmed the activity of the as prepared catalyst and the enhancement role of CuO co-catalyst.

In order to test the stability of the catalyst, recycling experiments were carried out. As can be seen in Figure S3, the catalyst showed strong photocatalytic ability for the degradation of MO for threes cycles. The catalyst was separated by centrifugation after every run and washed with deionized water for several times. We observed a decrease in reactivity after every run which may be because of the mass loss of catalyst during washing and centrifugation[29].

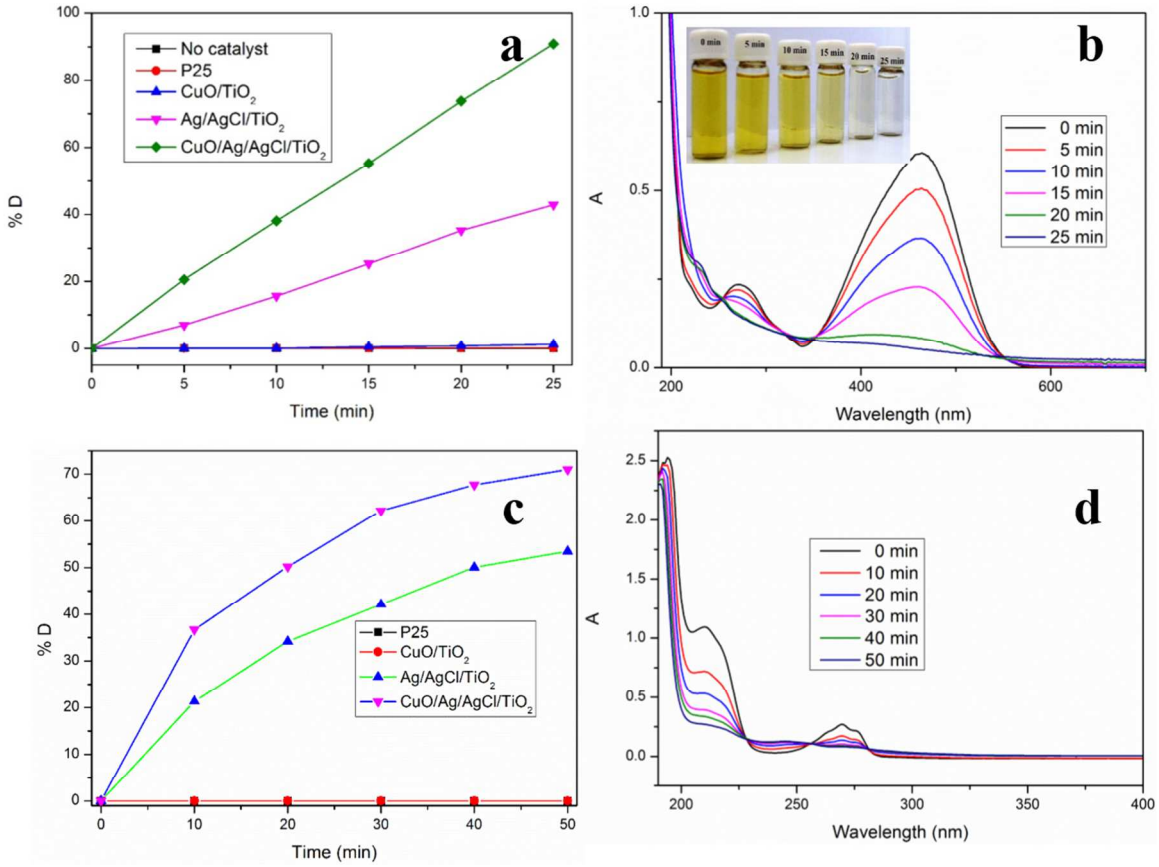

Figure 4: (a) Photocatalytic degradation of MO by various materials, (b) Change in MO concentration with irradiation time, (c) Photocatalytic degradation of phenol by various materials, and (d) Change in phenol concentration with irradiation time.

3.4 Mechanism for enhanced photocatalytic activity

There are different factors which can influence the photocatalytic activity of TiO_2[2]. Among those, band gap tuning of TiO_2 is considered to be a key factor to improve the visible light photocatalysis[30], and the band gap of TiO_2 can be effectively modified by

doping[7]. In order to investigate the effect of Ag, CuO, and Ag/AgCl on TiO_2 band gap in our study, we calculated the band gap of TiO_2 by using Einstein's energy equation[31]

$$E_g^{nano} = hc/\lambda$$

As can be seen in Figure S2, the band gaps in the case of Ag/TiO_2 (2.30 eV) and CuO/TiO_2 (2.36 eV) correspond to the visible region of the spectrum, however, they showed no visible light activity, while TiO_2 band gaps in the case of $Ag/AgCl/TiO_2$ (3.07 eV) and $CuO/Ag/AgCl/TiO_2$ (3.13 eV) correspond to the near UV region, but they showed very high visible light activity. From these results, we speculate that band gap tuning played very little role for the visible light activity of TiO_2 in our experiments. Hence we tried to explore the other possible factors which can play major role in the visible light photocatalytic activity of $CuO/Ag/AgCl/TiO_2$.

As mentioned above, CuO/TiO_2 showed no photocatalytic activity under our experimental conditions (Figure 4a) even though light was absorbed by CuO/TiO_2 in the visible region (Figure 3). Qui et al.[32] showed that the crystalline Cu(II) is photocatallytically inactive, however, Cu(II) species in nanoclusters are very efficient for the visible light photocatalysis of TiO_2. Absence of Cu(II) nanoclusters may be the reason for no photocatalytic activity by CuO/TiO_2 in our experiments.

Silver NPs can absorb considerable amount of energy from the visible light owing to their SPR. Semiconductor photocatalysis can be initiated by the SPR either by direct hot electron transfer from the plasmonic NPs into the CB of semiconductor or by transferring plasmonic energy to excite charges inside the semiconductor[33]. These photoexcited charges are responsible for the photocatalysis. Prior to light irradiation, the photocatalyst is kept under dark in a solution of dye or organic pollutant. The dye molecules get adsorbed onto the surface of the photocatalyst thus providing active sites for the oxidation of holes. Both the electrons and holes react with different surface species to bring the degradation of the organic pollutants.

AgCl proved to be very vital for the visible light activity of CuO/Ag/AgCl/TiO_2. AgCl itself has a direct band gap of 3.25 eV and an indirect band gap of 5.2 eV[34] which suggests it should not be active under visible light. However, AgCl is photosensitive because of its point ionic defects and electron traps[35]. The role of AgCl in Ag/AgCl system has been explained by Wang et al.[18]. In short, the surface of AgCl is negatively charged because it is most likely terminated by Cl^- ions. As a result of this, the deposited Ag NPs on AgCl surface should experience a charge polarization in such a way that negative regions are away while positive regions are close to the Ag/AgCl interface. When visible light photons are absorbed by Ag NPs, they are efficiently separated into

electrons and holes in such a way that electrons move to the surface of Ag NPs away from the Ag/AgCl interface, while the holes move to the surface of AgCl particles bearing Ag NPs. Hence better separation of photoexcited species is achieved.

In order to better understand the role of AgCl for the visible light photocatalytic activity, Ag/TiO_2 was prepared by the same method with some modifications (SI). Although Ag/TiO_2 showed strong absorption in the visible region (Figure S1 b) but it showed no photocatalytic activity (Figure S1 c). Ag/TiO_2 does not show visible light degradation of pollutants because Ag NPs are very reactive and they form a layer of AgO when they are in direct contact with TiO_2[13, 36]. Furthermore, UV-Vis spectra of Ag/TiO_2 and $Ag/AgCl/TiO_2$ are clearly different from each other as shown in Figure S1 b. This difference suggests the changes in the SPR signals of Ag NPs. A possible explanation for this can be that the SPR of Ag NPs is very sensitive to the surrounding environment and the SPR peak shifts to the longer wavelength, away from the important spectral domains of the near-UV , if the surrounding material has a greater refractive index[13]. TiO_2 has a refractive index 2.45 and 2.7 for anatase and rutile phase, respectively[37], while the refractive index of AgCl is 2.07[38]. Hence AgCl also helps to achieve the more useful SPR response from Ag NPs.

To investigate the role of $Cu(NO_3)_2 \cdot 3H_2O$ concentration on the photocatalytic activity of $Ag/AgCl/TiO_2$, a series of experiments was carried out with varying the concentration of $Cu(NO_3)_2 \cdot 3H_2O$ at optimized reaction conditions. Different concentrations of $Cu(NO_3)_2 \cdot 3H_2O$ used were $1.25*10^{-5}$ mol L^-, $2.5*10^{-5}$ mol L^-, $5*10^{-5}$ mol L^-, $2*10^{-4}$ mol L^-, and $3*10^{-5}$ mol L^-, and the resultant $CuO/Ag/AgCl/TiO_2$ can be referred as $CuO/Ag/AgCl/TiO_2$ ($1.25*10^{-5}$ M), $CuO/Ag/AgCl/TiO_2$ ($2.5*10^{-5}$ M), $CuO/Ag/AgCl/TiO_2$ ($5*10^{-5}$ M), $CuO/Ag/AgCl/TiO_2$ ($2*10^{-4}$ M), and $CuO/Ag/AgCl/TiO_2$ ($3*10^{-5}$ M), respectively. The obtained photocatalysts were tested for the visible light photocatalysis and it was found that $2.5*10^{-5}$ mol L^- of $Cu(NO_3)_2 \cdot 3H_2O$ was the optimum amount for our experimental conditions to achieve the highest photocatalytic activity. When more $Cu(NO_3)_2 \cdot 3H_2O$ was added, the photocatalytic activity considerably decreased (Figure 5a). This is in good agreement with the reported co-catalyst modified photocatalysis for $Fe(III)/TiO_2$[39, 40] and $Cu(II)/TiO_2$[41]. An optimum amount of co-catalyst is required to achieve the maximum photocatalytic activity A further increase in co-catalyst amount may reduce the oxidation active sites for photogenerated holes at the surface of the photocatalyst, thus resulting in decreased activity[40].

Besides this explanation for the decreased photocatalytic activity with increasing co-catalyst amount, we observed an interesting phenomenon of the decrease in the SPR

peaks of Ag NPs at higher concentrations of $Cu(NO_3)_2 \cdot 3H_2O$. This can be seen in Figure 5b which shows the UV-Vis spectra of different catalysts with varying the amount of $Cu(NO_3)_2 \cdot 3H_2O$. A possible reason could be that at higher concentration of $Cu(NO_3)_2 \cdot 3H_2O$, more CuO particles are formed which can aggregate to form larger particles[42]. These larger CuO particles may cover the Ag NPs thus preventing the interaction of visible light and Ag NPs, hence a decrease in the SPR signals is resulted. With the decrease in the SPR signals, photocatalytic activity decreased accordingly.

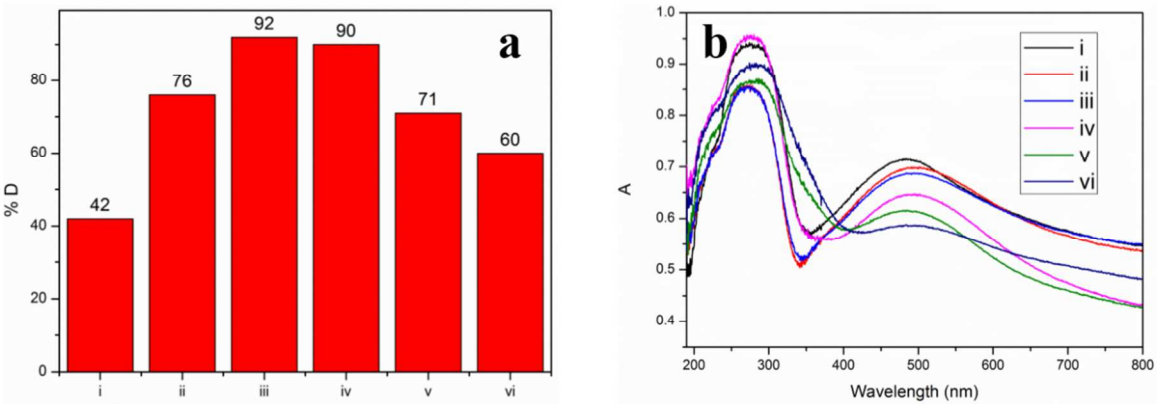

Figure 5: (a) Photocatalytic degradation of MO and (b) UV-Vis spectra of various catalysts: (i) $Ag/AgCl/TiO_2$, (ii) $CuO/Ag/AgCl/TiO_2$ ($1.25*10^{-5}$ M), (iii) $CuO/Ag/AgCl/TiO_2$ ($2.5*10^{-5}$ M), (iv) $CuO/Ag/AgCl/TiO_2$ ($5*10^{-5}$ M), (v) $CuO/Ag/AgCl/TiO_2$ ($2*10^{-4}$ M), and (vi) $CuO/Ag/AgCl/TiO_2$ ($3*10^{-5}$ M).

The photodegradation of organic pollutants have been reported by different reactive species such as h^+, $O_2^{-\bullet}$, and $OH^{\bullet}$[42, 43]. The role of individual reactive species is varied depending on the type of photocatalyst[44]. In order to better understand the mechanism of photodegradation of MO over CuO/Ag/AgCl/TiO_2 under visible light, we studied the photodegradation in the presence of different scavengers. We used TEA as h^+ scavengers[44, 45], *p*-benzoquinone as $O_2^{-\bullet}$ scavengers[46, 47], and *t*-butyl alcohol as $OH^{\bullet}$ scavengers[46, 47]. These scavengers were added to the MO solution along with the catalyst prior to the light irradiation. As shown in Figure 6, no photodegradation was achieved in the presence of TEA (1.25 mL) which suggests that photogenerated holes are the major reactive species in our experiments. We employed *p*-benzoquinone (1 mg) to evaluate the role of $O_2^{-\bullet}$ in the photocatalytic degradation of MO under our experimental conditions. The % degradation of MO decreased from 92% to 70% in the presence of *p*-benzoquinone suggesting that $O_2^{-\bullet}$ play lesser role in the photodegradation of MO. We used *t*-butyl alcohol (0.065 mL) to scavenge $OH^{\bullet}$. A small decrease of 5% in the photodegradation of MO suggests that $OH^{\bullet}$ species play a very little role in the overall degradation in our experiments.

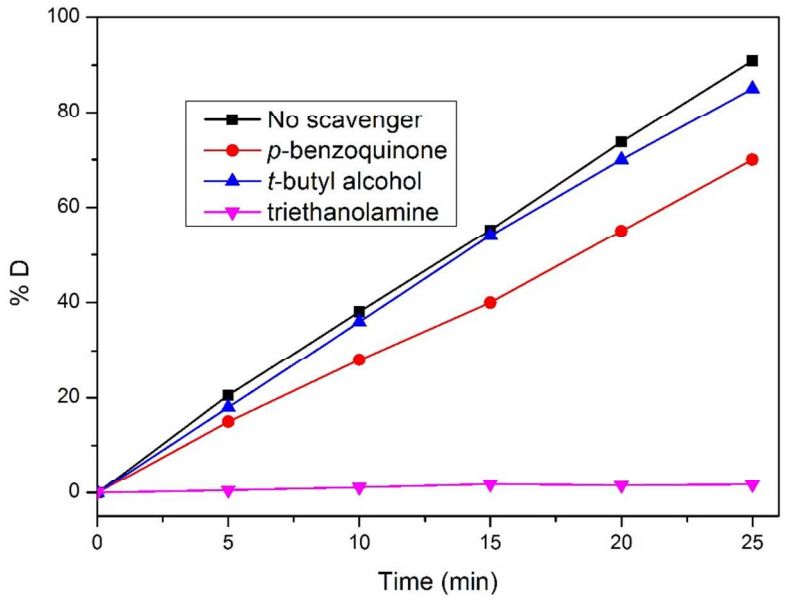

Figure 6: Photocatalytic degradation of MO over the CuO/Ag/AgCl/TiO_2 in the presence of scavengers.

The photocatalytic action of the CuO/Ag/AgCl/TiO_2 can be understood by the suggested mechanism in Figure 7. This mechanism is similar to the Ag/AgCl/TiO_2 mechanism proposed by Yu et al.[17] Under visible light irradiation, electron-hole pairs are formed in Ag NPs due to SPR. The excited electrons from Ag NPs can be injected into TiO_2 CB. The electrons in TiO_2 CB can readily react with O_2 which can lead the formation of reactive $O_2^{-\bullet}$ species. The photoexcited electrons from Ag NPs can inject into the TiO_2 CB due to Schottky barrier formed at the Ag/TiO_2 interface[48]. The Schottky barrier is formed due to the larger work function of Ag and the electric field in the space-charge layer could promote the injection of electrons form Ag surface to TiO_2 CB. On the other

hand, holes from Ag NPs react with Cl^- to form Cl° atoms[18] which are also very reactive species for the degradation of organic pollutants.

Ag NPs can also cause the direct transfer of plasmonic energy into TiO_2 which can lead to formation of electron-hole pairs in TiO_2[33]. This can result in formation of more electron-hole pairs. The electrons would react with the O_2 as proposed above, however, holes in this case can directly oxidize the pollutant molecule. CuO was found to highly enhance the photocatalytic degradation of MO and phenol (Figure 4a and c). As already mentioned, CuO can act as a co-catalyst[32]. As a co-catalyst, CuO enhances the photocatalytic activity of $Ag/AgCl/TiO_2$ by a two way action: (i) by absorbing the photoexcited electrons, thus acting as sink for electrons, which suppresses the recombination of electrons and holes. The photoexcited electrons can be absorbed from the conduction band of TiO_2 as well as they can be directly transferred from the valance band of TiO_2 by IFCT. As a result of this, more holes are available for the generation of $OH^{\bullet}$ radicals, hence enhanced photocatalytic degradation is achieved, (ii) electrons absorbed by CuO are transferred to O_2 which results in the formation of $O_2^{-\bullet}$ species, as depicted in Figure 7.

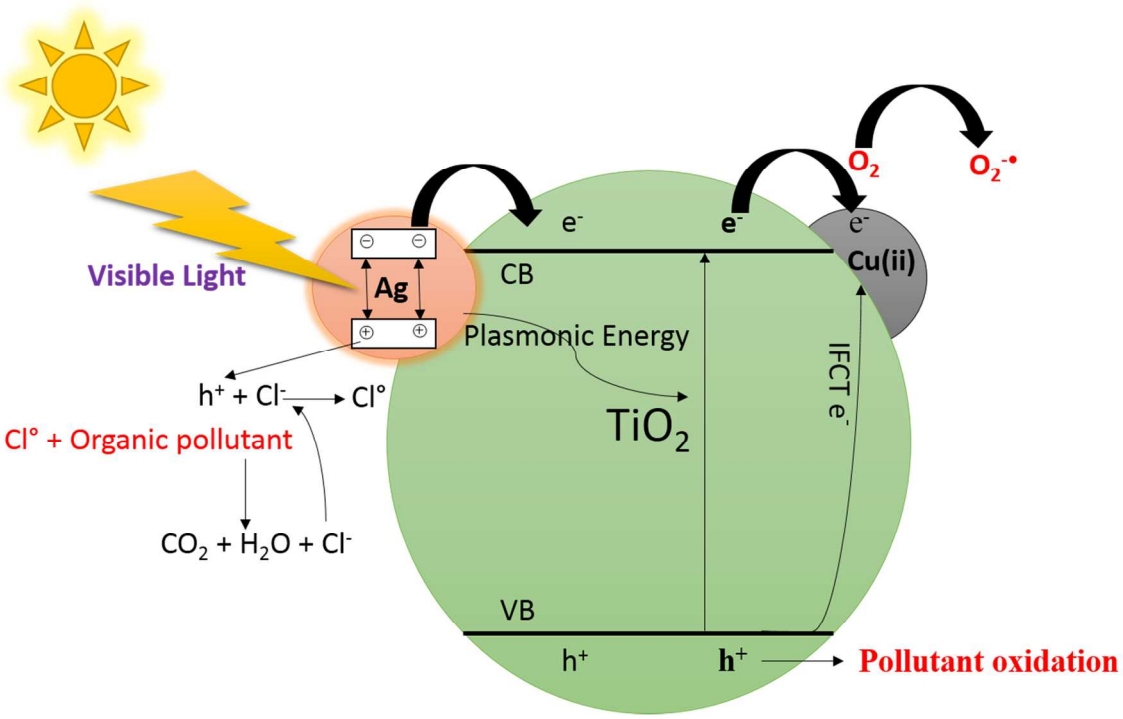

Figure 7: Schematic representation of the photocatalytic degradation of MO by CuO/Ag/AgCl/TiO_2.

4 Conclusions

In summary, the plasmonic catalyst CuO/Ag/AgCl/TiO_2 was fabricated via a reverse microemulsion synthesis. Role of CuO as a co-catalyst for Ag/AgCl/TiO_2 was studied. The photocatalytic degradation of MO and phenol under visible light was studied to evaluate the photocatalytic activity. SPR of Ag NPs was found to be the reason for the photocatalytic activity of the catalyst under visible light irradiation. AgCl proved to be vital to better utilize the SPR of Ag NPs. CuO is suggested to act as a sink for

photogenerated electrons which enhanced the photodegradation of MO and phenol by suppressing the charge recombination and also generating of $O_2^{-\bullet}$ species at the same time. The photocatalyst was found stable and easy to separate after photocatalysis. The use of CuO as a co-catalyst can be extended to the existing plasmon based TiO_2 photocatalysts to further enhance their activity.

Acknowledgments

This work is supported by the National Natural Science Foundation of China (Grants No. 21176038), the Science Fund for Creative Research Groups of the National Natural Scien ce Foundation of China (Grants No 21421005), the Ministry of Education Innovation Team (IRT-13R06), and Dalian University of Technology Innovation Team (DUT2013TB07).

Notes and References

Supporting information includes: Synthesis equations for $CuO/Ag/AgCl/TiO_2$; synthesis, XRD patterns, and UV-Vis spectrum for Ag/TiO_2; band gap calculations; and stability of the photocatalyst.

1. M. R. Hoffmann, S. T. Martin, W. Choi and D. W. Bahnemann, *Chem. Rev.*, 1995, **95**, 69-96.

2. X. Chen and S. S. Mao, *Chem. Rev.*, 2007, **107**, 2891-2959.

3. X. Chen, S. Shen, L. Guo and S. S. Mao, *Chem. Rev.*, 2010, **110**, 6503-6570.

4. B. G. O'Regan, Michael, *Nature*, 1991, **353**, 737-740.

5. A. L. Linsebigler, G. Lu and J. T. Yates, *Chem. Rev.*, 1995, **95**, 735-758.

6. T. Froschl, U. Hormann, P. Kubiak, G. Kucerova, M. Pfanzelt, C. K. Weiss, R. J. Behm, N. Husing, U. Kaiser, K. Landfester and M. Wohlfahrt-Mehrens, *Chem. Soc. Rev.*, 2012, **41**, 5313-5360.

7. L. Sang, Y. Zhao and C. Burda, *Chem. Rev.*, 2014, **114**, 9283-9318.

8. R. Asahi, T. Morikawa, T. Ohwaki, K. Aoki and Y. Taga, *Science*, 2001, **293**, 269-271.

9. P. V. Kamat and D. Meisel, *Curr. Opin. Colloid In*, 2002, **7**, 282-287.

10. S. Sakthivel and H. Kisch, *Angew. Chem., Int. Ed.*, 2003, **42**, 4908-4911.

11. R. Daghrir, P. Drogui and D. Robert, *Ind. Eng. Chem. Res.*, 2013, **52**, 3581-3599.

12. S. Liu, J. Yu and M. Jaroniec, *J. Am. Chem. Soc.*, 2010, **132**, 11914-11916.

13. K. Awazu, M. Fujimaki, C. Rockstuhl, J. Tominaga, H. Murakami, Y. Ohki, N. Yoshida and T. Watanabe, *J. Am. Chem. Soc.*, 2008, **130**, 1676-1680.

14. X. Zhou, G. Liu, J. Yu and W. Fan, *J. Mater. Chem.*, 2012, **22**, 21337-21354.

15. E. Thimsen, F. Le Formal, M. Grätzel and S. C. Warren, *Nano Lett.*, 2010, **11**, 35-43.

16. M. Rycenga, C. M. Cobley, J. Zeng, W. Li, C. H. Moran, Q. Zhang, D. Qin and Y. Xia, *Chem. Rev.*, 2011, **111**, 3669-3712.

17. J. Yu, G. Dai and B. Huang, *J. Phy. Chem. C*, 2009, **113**, 16394-16401.

18. P. Wang, B. Huang, X. Qin, X. Zhang, Y. Dai, J. Wei and M.-H. Whangbo, *Angew. Chem., Int. Ed.*, 2008, **47**, 7931-7933.

19. W. Zhou, H. Liu, J. Wang, D. Liu, G. Du and J. Cui, *ACS Appl. Mater. Interfaces*, 2010, **2**, 2385-2392.

20. C. Creutz, B. S. Brunschwig and N. Sutin, *J. Phys. Chem. B*, 2005, **109**, 10251-10260.

21. D. Wang, Y. Li, G. Li Puma, C. Wang, P. Wang, W. Zhang and Q. Wang, *Chem. Commun.*, 2013, **49**, 10367-10369.

22. X. Chen, L. Liu, P. Y. Yu and S. S. Mao, *Science*, 2011, **331**, 746-750.

23. J. Mendez-Ramos, P. Acosta-Mora, J. C. Ruiz-Morales, T. Hernandez, M. E. Borges and P. Esparza, *RSC Advances*, 2013, **3**, 23028-23034.

24. J. Yang, D. Wang, H. Han and C. Li, *Acc. Chem. Res.*, 2013, **46**, 1900-1909.

25. M. Liu, X. Qiu, M. Miyauchi and K. Hashimoto, *Chem. Mater.*, 2011, **23**, 5282-5286.

26. M. Liu, X. Qiu, M. Miyauchi and K. Hashimoto, *J. Am. Chem. Soc.*, 2013, **135**, 10064-10072.

27. M. Dahl, Y. Liu and Y. Yin, *Chem. Rev.*, 2014, **114**, 9853-9889.

28. Y. Yang, G. Zhang and W. Xu, *J. Colloid Interf. Sci*, 2012, **376**, 217-223.

29. Y. Shi, K. Zhou, B. Wang, S. Jiang, X. Qian, Z. Gui, R. K. K. Yuen and Y. Hu, *J. Mat. Chem. A*, 2014, **2**, 535-544.

30. J. Schneider, M. Matsuoka, M. Takeuchi, J. Zhang, Y. Horiuchi, M. Anpo and D. W. Bahnemann, *Chem. Rev.*, 2014, **114**, 9919-9986.

31. A. S. Bhadwal, R. M. Tripathi, R. K. Gupta, N. Kumar, R. P. Singh and A. Shrivastav, *RSC Advances*, 2014, **4**, 9484-9490.

32. X. Qiu, M. Miyauchi, K. Sunada, M. Minoshima, M. Liu, Y. Lu, D. Li, Y. Shimodaira, Y. Hosogi, Y. Kuroda and K. Hashimoto, *ACS Nano*, 2011, **6**, 1609-1618.

33. S. K. Cushing, J. Li, F. Meng, T. R. Senty, S. Suri, M. Zhi, M. Li, A. D. Bristow and N. Wu, *J. Am. Chem. Soc.*, 2012, **134**, 15033-15041.

34. J. Tejeda, N. J. Shevchik, W. Braun, A. Goldmann and M. Cardona, *Phys. Rev. B*, 1975, **12**, 1557-1566.

35. J. F. Hamilton, *Photogr. Sci. Eng.*, 1974, **18**, 493-500.

36. X. Zhang, Y. Zhu, X. Yang, S. Wang, J. Shen, B. Lin and C. Li, *Nanoscale*, 2013, **5**, 3359-3366.

37. P. Tao, Y. Li, A. Rungta, A. Viswanath, J. Gao, B. C. Benicewicz, R. W. Siegel and L. S. Schadler, *J. Mater. Chem.*, 2011, **21**, 18623-18629.

38. P. Patnaik, *Handbook of Inorganic Chemicals*, McGraw-Hill, 2003.

39. H. Yu, H. Irie, Y. Shimodaira, Y. Hosogi, Y. Kuroda, M. Miyauchi and K. Hashimoto, *J. Phy. Chem. C*, 2010, **114**, 16481-16487.

40. H. Yu, L. Xu, P. Wang, X. Wang and J. Yu, *Appl. Catal., B*, 2014, **144**, 75-82.

41. P. Wang, Y. Xia, P. Wu, X. Wang, H. Yu and J. Yu, *J. Phy. Chem. C*, 2014, **118**, 8891-8898.

42. J. Xiong, Z. Li, J. Chen, S. Zhang, L. Wang and S. Dou, *ACS Appl. Mater. Interfaces*, 2014, **6**, 15716-15725.

43. M. Yin, Z. Li, J. Kou and Z. Zou, *Environ. Sci. Technol.*, 2009, **43**, 8361-8366.

44. L. Chen, R. Huang, S.-F. Yin, S.-L. Luo and C.-T. Au, *Chem. Eng. J.*, 2012, **193–194**, 123-130.

45. Q. Yuan, L. Chen, M. Xiong, J. He, S.-L. Luo, C.-T. Au and S.-F. Yin, *Chem. Eng. J.*, 2014, **255**, 394-402.

46. Y. Lin, D. Li, J. Hu, G. Xiao, J. Wang, W. Li and X. Fu, *J. Phy. Chem. C*, 2012, **116**, 5764-5772.

47. H. Katsumata, T. Sakai, T. Suzuki and S. Kaneco, *Ind. Eng. Chem. Res.*, 2014, **53**, 8018-8025.

48. K. Kawahara, K. Suzuki, Y. Ohko and T. Tatsuma, *Phys. Chem. Chem. Phys.*, 2005, **7**, 3851-3855.

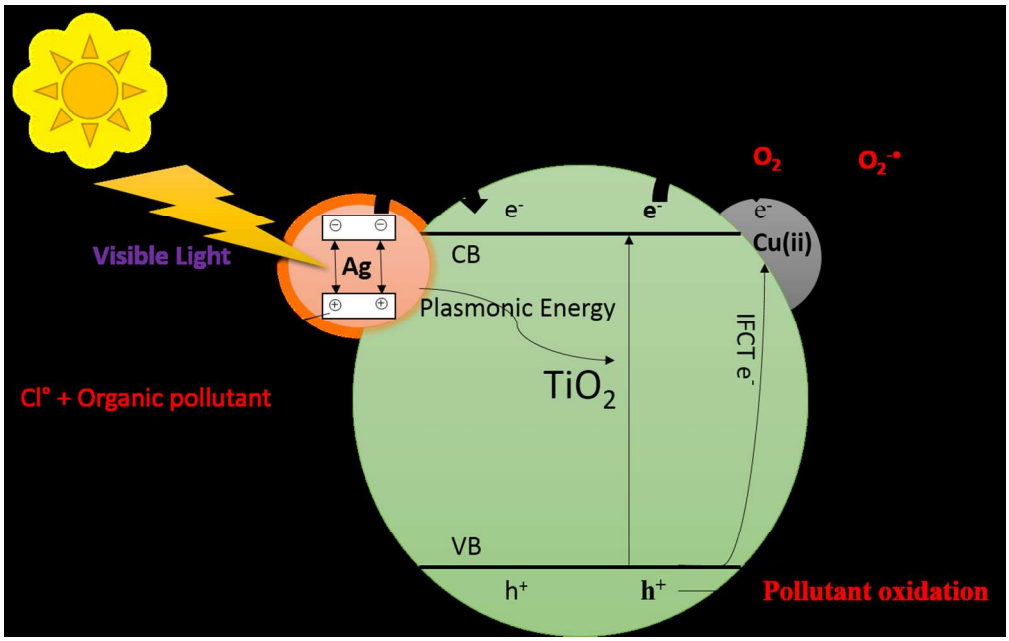

230x145mm (150 x 150 DPI)